Multiferroic phase diagram of Y partially substituted $Dy_{1-x}Y_xMnO_3$

N. Zhang,[1] S. Dong,[2] G. Q. Zhang,[1] L. Lin,[1] Y. Y. Guo,[1] J.-M. Liu,[1,3,a)] and Z. F. Ren[4]
[1]*Laboratory of Solid State Microstructures, Nanjing University, Nanjing 210093, People's Republic of China*
[2]*Department of Physics, Southeast University, Nanjing 211189, People's Republic of China*
[3]*International Center for Materials Physics, Chinese Academy of Sciences, Shenyang 110016, People's Republic of China*
[4]*Department of Physics, Boston College, Chestnut Hill, Massachusetts 02467, USA*

(Received 22 November 2010; accepted 20 December 2010; published online 7 January 2011)

The effect of nonmagnetic Y partial substitution at the Dy site in $Dy_{1-x}Y_xMnO_3$ up to $x=0.2$ on magnetism, specific heat, and ferroelectricity is investigated, which resulted in a preliminary multiferroic phase diagram. It is revealed that the Y partial substitution suppresses the Dy-spin ordering point (T_{Dy}) and ferroelectric ordering point (T_{FE}) but enhances the Mn-spin ordering point (T_N). The interaction between the spins of Dy and Mn is remarkably affected by Y substitution. The measured electrical polarization depends on the Y substitution in a complex way because the ferroelectricity is sensitive to the interaction between the spins of Dy and Mn. © *2011 American Institute of Physics*. [doi:10.1063/1.3536506]

Multiferroics, in which magnetism and ferroelectricity coexist and are mutually coupled, have received attention due to the fascinating physics and potential applications.[1] In particular, the orthorhombic ABO_3-type manganites $RMnO_3$ (R is trivalent rare-earth ion) with their strongly coupled spin and ferroelectric orders and rich phase diagrams have been extensively investigated.[2–12] Cross coupling between ferroelectricity and magnetism can be realized in these manganites, in which Mn spins in a cycloidal configuration that can simultaneously break the spatial inversion and time-reversal symmetries, and the ferroelectricity originates from the complex Mn-spin orders.[3,13] One of the mechanisms for ferroelectricity generation is associated with the noncollinear spiral spin (NSS) order, and the inverse Dzyaloshinskii-Moriya interaction or the spin current scenario induces the ferroelectric polarization P below temperature $T=T_{FE}$, the ferroelectric ordering point.[14]

Regarding this mechanism, the possible contribution of the R spin ordering to P, if any, is usually ignored.[15,16] However, recent studies revealed that the R spin ordering also plays substantial roles in modulating P, as identified particularly in $DyMnO_3$ (DMO).[5–11] The Mn sublattice polarizes the Dy spins with propagation vector at the Mn order, τ^{Mn}.[6–9] The Dy-spin order—apart from the maximal $2.5\mu_B$ moment along the b axis—carries a small induced moment along the c axis even close to the Mn antiferromagnetic (AFM) ordering point T_N, i.e., above T_{FE}.[6,7] At $T<T_{FE}$, the inversion-symmetry breaking in DMO is accomplished not by the Mn NSS ordering alone but also the Dy-4f spin cycloidal ordering.[8] This indicates a strong interaction J_{Mn-Dy} between the Mn-3d spins and the Dy-4f spins in both sinusoidal and cycloidal phases. A nonzero J_{Mn-Dy} thus brings in a so-called induced Dy-spin ordering accompanied by the Mn-spin ordering below T_N, giving rise to major shift in P for DMO below T_{FE}. However, this induced Dy-spin ordering only occurs above T_{Dy}, the point for the independent Dy-spin ordering with vector $\tau^{1/2}$. The rationale is that the interaction J_{Mn-Dy} is insufficient to overcome the independent Dy-spin ordering below T_{Dy}, which specifically leads to the suppression of the original incommensurate spiral Mn-spin order, again via the interaction J_{Mn-Dy}, inducing severe suppression of P below T_{Dy}.[5–7] Interestingly, the induced Dy-spin ordering, driven by magnetic field (H), can reemerge at $T<T_{Dy}$, indicating that P can be enhanced by an applied H.[5–7]

With the interaction J_{Mn-Dy} potentially a crucial factor to influence the multiferroicity of DMO, further investigation into its modulation and hence the multiferroicity is significant. While partial substitution at the Mn site has been tried and indicated a strong impact upon the induced Dy-spin ordering between $T_{Dy}\leq T\leq T_{FE}$,[10,11] a drawback of such partial substitution is that it mars the perfectness of the Mn-spin ordering. If a nonmagnetic partial substitution at the A site (Dy) is possible, with little change to the lattice symmetry and pristine structure, the interaction J_{Mn-Dy} can be more finely modulated. Y partial substitution for Dy seems to meet such a criterion. Nevertheless, the Dy spin is unfortunately hard to detect using neutron scattering due to large cross-sectional absorption.[7] As a solution to this dilemma, we propose to probe alternative characterizations to shed some light on partial substitution effects associated with the J_{Mn-Dy} modulation and multiferroicity in $Dy_{1-x}Y_xMnO_3$ (DYMO). In this work, through various measurements on DYMO, we demonstrate that the spin orders of Mn and Dy and their coupling as well as the multiferroicity can all be modulated effectively by partial substitution of Y for Dy. It should be noted that our motivation on DYMO is different from the widely studied $Eu_{1-x}Y_xMnO_3$.[4] Our focus is on the modulation of the magnetic interaction between the spins of A site and B site.

Polycrystalline $Dy_{1-x}Y_xMnO_3$ samples ($0\leq x\leq 0.2$) were synthesized by solid state reaction. The phase purity and crystallinity were checked by x-ray diffraction (XRD) using Cu $K\alpha$ radiation. Magnetization (M) and specific heat (C/T) measurements were performed using the Quantum Design superconducting quantum interference device magnetometer and physical property measurement system (PPMS), respectively. The dielectric constant (ε) was determined by HP4294A impedance analyzer in PPMS. For measuring polarization P, the details of the measuring procedure were reported earlier.[16]

a)Electronic mail: liujm@nju.edu.cn.

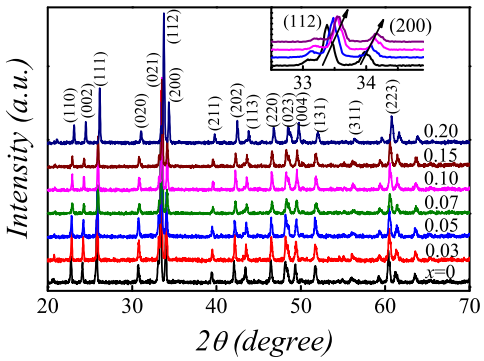

FIG. 1. (Color online) XRD θ-2 θ patterns for DYMO with $0 \le x \le 0.2$ measured at room temperature. The inset shows the (112) and (200) peaks for samples with $x=0$, 0.05, 0.10, and 0.15 from bottom to up.

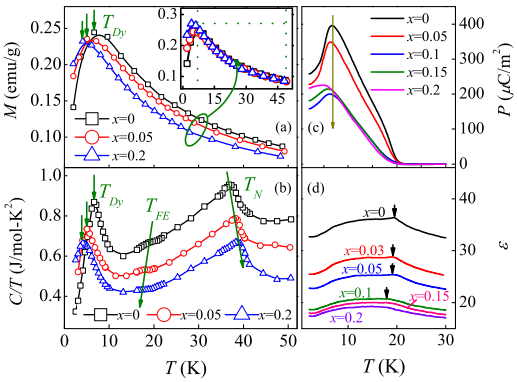

FIG. 3. (Color online) (a) Measured M and (b) C/T as a function of T for samples with $x=0$, 0.05, and 0.2. (c) Measured P and (d) ε as a function of T for DYMO with x varying from 0 to 0.2, respectively.

First, we identify the crystallinity of the DYMO samples by θ-2θ XRD patterns at room temperature, as shown in Fig. 1. The peaks suggest that the samples are well crystallized and can be indexed by single orthorhombic structure with space group *Pbnm*. A continuous but slight shift of the peaks toward higher 2 θ with increasing x is observed (inset of Fig. 1), indicating a slight lattice contraction due to the partial substitution.

Subsequently, we characterized the magnetic and ferroelectric properties. As a reference, we first show in Figs. 2(a) and 2(b) the measured data on M, C/T, ε, and P as a function of T for DMO. The M-T curve in the zero-field-cooled (ZFC) condition exhibits a peak at $T=T_{\mathrm{Dy}} \sim 6.5$ K due to the independent Dy-spin ordering. No clear signature of the NSS ordering and incommensurate *lock-in* transition of Mn spins is observed due to the dominating paramagnetic susceptibility of the Dy spins which have a much larger moment than Mn spins. We thus turn to the C/T data and observed a sharp anomaly at $T_N \sim 37$ K corresponding to the onset of a collinear sinusoidal Mn-spin ordering with an incommensurate wave vector. A minor second anomaly at $T=T_{FE} \sim 19$ K signatures the Mn NSS ordering plus the induced Dy NSS ordering with a T-independent wave vector at which a nonzero P is observed. Upon further cooling down to $T=T_{\mathrm{Dy}} \sim 6.5$ K, a third major anomaly of C/T associated with the independent Dy-spin ordering is identified, consistent with the peak positions in the M-T and P-T curves. These successive phase transitions are in agreement with earlier reports.[5–9]

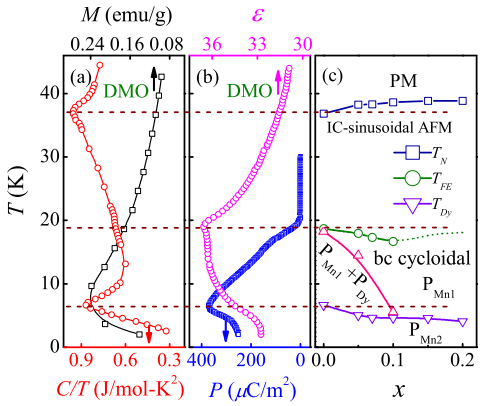

FIG. 2. (Color online) (a) Measured M and (C/T) and (b) measured P and ε as a function of T for DMO. The multiferroic phase diagram of DYMO with $0 \le x \le 0.2$ is presented in (c), where PM, IC, and AFM denote the paramagnetic, incommensurate, and antiferromagnetic spin orders, respectively. P_{Mn1}, P_{Mn2}, and P_{Dy} represent the contributions to P from the Mn NSS orders with different propagate vectors and the Dy NSS ordering, respectively.

Built on the study on DMO, we proceeded to DYMO. Figure 2(c) shows a rough multiferroic phase diagram in the (T-x) space. In brief, T_N increases with x while both T_{FE} and T_{Dy} decrease. It clearly shows the substantial impact of the Y partial substitution for Dy on the magnetic and ferroelectric properties. In particular, the response of T_{FE} to the substitution clearly indicates an achievement of the variation in the interaction $J_{\mathrm{Mn-Dy}}$.[6–8]

Based on the phase diagram shown in Fig. 2(c), we look into the details of the effect of the Y partial substitution and the data are shown in Figs. 3(a)–3(d). First, the measured M-T curves for samples with $x=0$, 0.05, and 0.2 [Fig. 3(a)] show that the AFM transition occurring at T_{Dy} downshifts gradually with increasing x. The measured M signals above T_{Dy} are mainly induced by Dy spins whose moment ($\sim 10\mu_B$) is much larger than that of Mn spins ($\sim 4\mu_B$).[6,9] The dilution effect from the Y partial substitution validates this. To multiply the magnetization curves by a dilution factor $f=[(x\cdot \mathrm{Y}+(1-x)\mathrm{Dy}+\mathrm{Mn}+3\mathrm{O})/[(1-x)(\mathrm{Dy}+\mathrm{Mn}+3\mathrm{O})]$, where Y, Dy, Mn, and O represent the formula weight of these elements in DYMO, it can be seen that all the recalculated magnetization curves above T_{Dy} almost fall on the same master curve, as shown in the inset of Fig. 3(a). Hence, no anomaly in the M-T curves can be observed in connection with the AFM transitions of Mn spins at T_N as potential anomaly is merged by the contribution from Dy-spin moments.

Figure 3(b) shows the measured $C/T \sim T$ curves for the three samples. As expected, T_{Dy} decreases with x due to the dilution of the Dy-spin sublattice by the Y partial substitution. For $T_N(x)$, it is known that $YMnO_3$ has its $T_N \sim 42$ K,[4] which is higher than that of DMO. The variation in $T_N(x)$ can thus be understood from the strong dependence of $J_{\mathrm{Mn-Dy}}$ on x. It is this interaction that allows the induced Dy-spin ordering above T_{Dy}, implying that $J_{\mathrm{Mn-Dy}}$ weakens the AFM Mn-spin interaction. In other words, the AFM Mn-spin ordering has to expend part of its energy to compensate the energy required for the induced Dy-spin ordering due to the nonzero $J_{\mathrm{Mn-Dy}}$. Therefore, a dilution of Dy-spin sublattice by Y partial substitution suppresses $J_{\mathrm{Mn-Dy}}$, which then allows the AFM ordering of Mn spins at a higher T, resulting in the gradual increase in T_N with x.

As mentioned above, T_{FE} signatures the Mn NSS ordering plus the induced Dy NSS ordering, which together result in nonzero P.[8] Since the induced Dy-spin order has the same propagation vector as that of the Mn order (i.e., τ^{Mn}), the symmetric exchange striction between the two spin sublattices may contribute to the enhancement of P.[12] A dilution of Dy-spin sublattice by the Y partial substitution partially breaks the Dy NSS order, thus resulting in decrease in T_{FE}, as shown in Fig. 3(b). This is also confirmed by the anomaly in $\varepsilon(T)$ shown in Fig. 3(d). Meanwhile, a substantial suppression of P, also expected, is demonstrated by the P-T data shown in Fig. 3(c). The P-T curve downshifts drastically with increasing x until $x\sim0.1$. In contrast, at $0.1<x<0.2$, the P-T data above T_{Dy} no longer show significant suppression with increasing x. Therefore, at $x>0.1$, the induced Dy NSS order between T_{Dy} and T_{FE} has probably been completely melted away and there is no more contribution to P.

Nevertheless, intricacies are embedded in the $x>0.1$ samples. Apparently a higher Y partial substitution not only melts away the induced Dy NSS order between $T_{\mathrm{Dy}}<T<T_{FE}$ but also damages the independent Dy-spin order below T_{Dy}, thus partially lifting the suppression of polarization P below T_{Dy}. This explains why the measured P below T_{Dy} is enhanced with increasing x at $x>0.1$, although it still decreases with decreasing T below T_{Dy}. It can thus be inferred that the measured P below T_{FE} consists of several components: (1) P_{Mn1}, from the Mn NSS order with vector $\tau^{\mathrm{Mn1}}=0.385b$, which is always found between $T_{\mathrm{Dy}}<T<T_{FE}$; (2) P_{Dy}, from the Mn-induced Dy NSS order with the same $\tau^{\mathrm{Mn1}}=0.385b$,[6–8] which is gradually suppressed by the Y partial substitution until $x\sim0.1$ and phases out above $x\sim0.1$ (P_{Dy} has the same sign as P_{Mn1}); and (3) P_{Mn2}, from the modulated Mn NSS order with $\tau^{\mathrm{Mn2}}=0.405b$.[9,12] The third component is present only below T_{Dy} since the original incommensurate spiral Mn-spin structure ($\tau^{\mathrm{Mn1}}=0.385b$) is suppressed by the independent Dy-spin ordering; however, it is gradually enhanced with x above $x\sim0.1$ since the independent Dy-spin order is damaged by the Y partial substitution.

Consequently, the measured P is the sum of the three components: $P=P_{\mathrm{Mn1}}+P_{\mathrm{Dy}}+P_{\mathrm{Mn2}}$. Incrementing additional data to the phase diagram is illuminating. As shown in Fig. 2(c), the polarization measured above T_{Dy} and represented by the upper triangles connects a boundary line to separate the two different regions: that with $P_{\mathrm{Mn1}}+P_{\mathrm{Dy}}$ below the line and that with P_{Mn1} above the line. Below T_{Dy}, P_{Mn1} and P_{Dy} disappear and the measured P is P_{Mn2}. It is worth mentioning that in both regions, each component itself also varies with x and T.

Since it is the induced Dy-spin order that is mainly responsible for the enhancement of P in DMO, a magnetic field modulation of P can be expected. The measured P-T curves under several H for samples $x=0$ and 0.1 are shown in Figs. 4(a) and 4(b), respectively. The data on DMO agree with previous reports.[5] As for samples with $x=0.1$, although the induced Dy-spin order is melted away by the Y partial substitution, a slight enhancement of P is observed under intermediate H at low T, as seen in Fig. 4(b). This can be understood by reference to the reemergence of the induced Dy-spin ordering which accompanies the suppression of the independent Dy-spin ordering under intermediate H at low T.[5–7] It is therefore reasonable to observe weaker enhancement of P in DYMO than in DMO, as shown in the inset of Fig. 4(a). Moreover, the magnetoelectric coefficient, defined as $\mathrm{ME}=[P(0)-P(H)]/P(0)$, at $T=2$ K and $H=9$ T is found to be enhanced from ~27% for samples with $x=0$ to ~50% for samples with $x=0.1$. The mechanism of this enhancement is that the stability of the NSS Mn- and Dy-spin orders is disturbed by the Y substitution, which facilitates the breaking of the NSS configuration by magnetic field, resulting in a stronger modulation of P by H in DYMO ($x=0.1$) than in DMO ($x=0$).

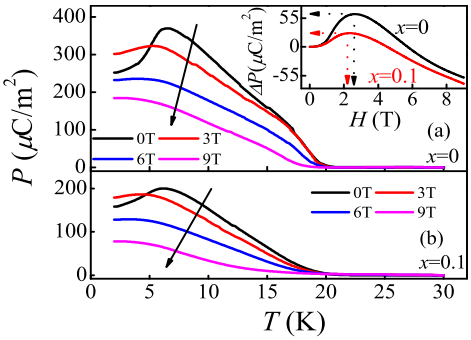

FIG. 4. (Color online) Measured P as a function of T under various H for samples with (a) $x=0$ and (b) $x=0.1$. The inset of (a) shows the P-H dependence at $T=2$ K for samples with $x=0$ and 0.1.

This work was supported by the Natural Science Foundation of China (Grant Nos. 50832002, 11004027, and 10874075) and the National Key Projects for Basic Research of China (Grant Nos. 2011CB922101 and 2009CB623303).

[1]M. Fiebig, J. Phys. D **38**, R123 (2005); W. Eerenstein, N. D. Mathur, and J. F. Scott, Nature (London) **442**, 759 (2006); S.-W. Cheong and M. Mostovoy, Nature Mater. **6**, 13 (2007); K. F. Wang, J.-M. Liu, and Z. F. Ren, Adv. Phys. **58**, 321 (2009).
[2]T. Kimura, T. Goto, H. Shintani, K. Ishizaka, T. Arima, and Y. Tokura, Nature (London) **426**, 55 (2003).
[3]M. Kenzelmann, A. B. Harris, S. Jonas, C. Broholm, J. Schefer, S. B. Kim, C. L. Zhang, S.-W. Cheong, O. P. Vajk, and J. W. Lynn, Phys. Rev. Lett. **95**, 087206 (2005).
[4]J. Hemberger, F. Schrettle, A. Pimenov, P. Lunkenheimer, V. Yu. Ivanov, A. A. Mukhin, A. M. Balbashov, and A. Loidl, Phys. Rev. B **75**, 035118 (2007).
[5]T. Kimura, G. Lawes, T. Goto, Y. Tokura, and A. P. Ramirez, Phys. Rev. B **71**, 224425 (2005).
[6]O. Prokhnenko, R. Feyerherm, E. Dudzik, S. Landsgesell, N. Aliouane, L. C. Chapon, and D. N. Argyriou, Phys. Rev. Lett. **98**, 057206 (2007).
[7]R. Feyerherm, E. Dudzik, A. U. B. Wolter, S. Valencia, O. Prokhnenko, A. Maljuk, S. Landsgesell, N. Aliouane, L. Bouchenoire, S. Brown, and D. N. Argyriou, Phys. Rev. B **79**, 134426 (2009).
[8]E. Schierle, V. Soltwisch, D. Schmitz, R. Feyerherm, A. Maljuk, F. Yokaichiya, D. N. Argyriou, and E. Weschke, Phys. Rev. Lett. **105**, 167207 (2010).
[9]R. Feyerherm, E. Dudzik, N. Aliouane, and D. N. Argyriou, Phys. Rev. B **73**, 180401(R) (2006).
[10]N. Zhang, K. F. Wang, S. J. Luo, T. Wei, X. W. Dong, S. Z. Li, J. G. Wan, and J.-M. Liu, Appl. Phys. Lett. **96**, 252902 (2010).
[11]O. Prokhnenko, N. Aliouane, R. Feyerherm, E. Dudzik, A. U. B. Wolter, A. Maljuk, K. Kiefer, and D. N. Argyriou, Phys. Rev. B **81**, 024419 (2010).
[12]R. Feyerherm, E. Dudzik, O. Prokhnenko, and D. N. Argyriou, J. Phys.: Conf. Ser. **200**, 012032 (2010).
[13]M. Mostovoy, Phys. Rev. Lett. **96**, 067601 (2006).
[14]I. A. Sergienko and E. Dagotto, Phys. Rev. B **73**, 094434 (2006); H. Katsura, N. Nagaosa, and A. V. Balatsky, Phys. Rev. Lett. **95**, 057205 (2005).
[15]S. Dong, R. Yu, S. Yunoki, J.-M. Liu, and E. Dagotto, Phys. Rev. B **78**, 155121 (2008); Q. C. Li, S. Dong, and J.-M. Liu, *ibid.* **77**, 054442 (2008).
[16]S. J. Luo, K. F. Wang, S. Z. Li, X. W. Dong, Z. B. Yan, H. L. Cai, and J.-M. Liu, Appl. Phys. Lett. **94**, 172504 (2009).